# Point-to-Point Channel Modelling Within Offshore Wind Farms

Joseph Mbogo, Xiao-Hong Peng and Zuoyin Tang

School of Engineering & Applied Science, Aston University, Birmingham, UK
mbogojm@aston.ac.uk, x-h.peng@aston.ac.uk and z.tang1@aston.ac.uk

**Abstract.** From the perspective of several measurement campaigns in the offshore environment, it has been reported that the sea surface reflections are the main source of deep fading. We present a novel solution to this problem, by investigating the analytical implications of the propagation model which best fits the offshore channel characteristics. We also present a novel and yet simple implementation of receiver diversity which can mitigate the fading caused by sea surface reflections and ensure that the link is always steady even under extreme turbulent conditions.

**Keywords:** Maritime Communications, Sea Surface Reflections, Channel Modelling, Long Range WLAN, Spatial Diversity.

## 1 Introduction and Motivation

Wireless Turbine-to-Turbine communications in a wind farm can greatly enhance the efficiency of the data acquisition process by decoupling the wind farm from the wired grid network architecture. In a nutshell, turbines can share meteorological information and other safety data much faster, which implies that an individual node can monitor itself as well as its neighbours. Advancement in wireless sensor networks has shown that most offshore platforms implementation will prefer wireless sensor motes to other electromechanical options [1]. Beyond Supervisory Control and Data Acquisition (SCADA), the turbine can provide a dual purpose service in the offshore environment. Apart from providing the valuable renewable energy, the turbine can share its wireless connection to the site maintenance staff, enabling them to control individual turbines while on site with their hand-held computers. There is also a big motivation for network service providers to utilise turbines as network access points or base stations to provide coverage to the vast oceans, avoiding the huge costs and latency issues from the current oceanic communication systems based on satellite networks [2].

### 1.1 Challenges of Signal Propagation within Offshore Environments

A wireless point-to-point link between any two offshore wind turbines presents some unique challenges which are not experienced on land. The main factors which directly affect the propagation of radio waves include: ducting, tidal waves, surface turbulence and sea-surface reflections. In particular, the sea-surface reflections exhibits the most detrimental effect on the propagation of radio signals in this environment. This is because the sea-surface acts as an electrical conductor for all radio frequency [3], which means that all incident Electromagnetic energy at radio frequency is mostly scattered by the sea-surface causing significant deep fades when the scattered Non-Line-of-Sight (NLOS) path interacts destructively with the Line-Of-Sight (LOS) path . The presence of tidal waves makes the height of an antenna above the sea-surface vary gradually causing periodic variations in the wireless channel. This results in a phenomena called tidal-fading [4], which is never experienced on land. Tidal fading in the offshore environment is not as detrimental as experienced near the shore and it changes slowly following the lunar orbits around the earth [5]. On the other hand extreme surface turbulence such as rogue waves are usually instantaneous and random, presenting a challenge to the overall turbine structural integrity [6]. In general sea surface reflections are an ever-present scenario and greatly depend on the height of the nodes which is largely affected by oceanic wave motion [7].

### 1.2 Related Work

The propagation of radio waves between individual offshore wind turbines has not been extensively investigated. However, there are several results in the reported literature that attempt to address this issue. The investigation by *Salehinejad et al.*, [8] on channel modelling between two offshore wind turbines, is closely related to the work on this topic. In this work, the model presented was based on ultra wide band communications using pulse position modulation. The data rate was limited to 10 *kbps* and the point-to-point node separation distance was up to 1 *km*. The key objective for the proposed model was a simple design of a low implementation cost. Their key contribution was the analysis of wide band signal propagation between two offshore wind turbines. The authors in [9], gave a survey of possible turbine-to-turbine communication technology but did not mention a viable wireless solution.

Other investigations into Offshore wind farm communication networks, were focused on the internetwork of wireless sensor motes [1]. A series of investigations reported by the same research team have also contributed to building a resilient network to support offshore wind farms [10] [11] which mainly focused on wired network topologies with simulation investigations developed in [10] where a single point-to-point microwave link between the wind farm and the control centre was setup.

## 2 Approach to Counteracting Sea Surface Reflections

Measurement campaigns by several research groups, including [12], [13] and [7], illustrated that the fading in the offshore environment can be better predicted using the two-ray model. In this section, we propose a novel diversity approach which could counteract deep fading due to surface reflections.

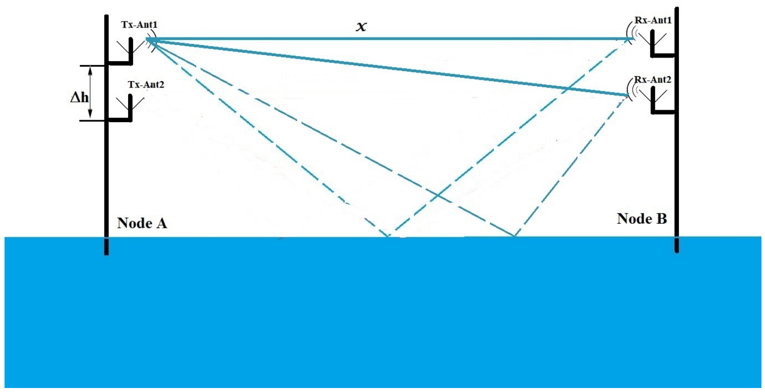


**Fig. 1.** $1 \times 2$ SIMO System to counteract sea surface Reflections

Consider an ideal case where the two nodes are perfectly identical, hence their antennas have the same gain ($\sqrt{G}$) and radiation pattern. Let the two antennas at node A be denoted by Tx-Ant1 placed at height $h_{A1}$ above the sea surface and Tx-Ant2 placed at height $h_{A2}$. Similarly the two receiver antennas at node B denoted by Rx-Ant1 placed at height $h_{B1}$ and Rx-Ant2 placed at height $h_{B2}$. Consider a simplex scenario where node A is transmitting with only Tx-Ant1 as depicted in fig 1 while node B in receiving mode can collect the incident waveforms from both its identical receivers vertically separated as shown in fig.1. The power received from antennas Rx-Ant1 and Rx-Ant2 can be estimated by equations (1) and (2) as $P_r1$ and $P_r2$ respectively from the generalised two-ray model under narrowband constraints [14].

$$P_r1 = P_t\left(\frac{c\sqrt{G}}{2\pi fx}\right)^2 \sin^2\frac{\pi f \Delta_x 1}{c} \tag{1}$$

$$P_r2 = P_t\left(\frac{c\sqrt{G}}{2\pi fx}\right)^2 \sin^2\frac{\pi f \Delta_x 2}{c} \tag{2}$$

where $P_t$ is the transmitted power in $(W)$, $c$ is the speed of electromagnetic waves in a vacuum, $G$ is the product of the antenna gains for both the transmitter and receiver, $x$ is the coverage distance between the transmitter and the receiver nodes, $f$ is the carrier frequency, $\Delta_x 1$ and $\Delta_x 2$ are the path differences of LOS and NLOS paths between Tx-Ant1 and the two receive antennas approximated from expressions (3 ) and (4 ) respectively [14].

$$\Delta_x 1 \approxeq \frac{2h_{A1}h_{B1}}{x} \tag{3}$$

$$\Delta_x 2 \approxeq \frac{2h_{A1}h_{B2}}{x} \tag{4}$$

Given that the receiver antennas are perfectly identical also in terms of the individual RF-chains, an equal gain combiner can be applied at node B, summing up the received power from equations (1) and (2), we can optimise the combined received power by controlling the phases of the received waveforms such that equation (5) holds.

$$\frac{\pi f \Delta_x 1}{c} = \frac{\pi f \Delta_x 2}{c} + \frac{\pi}{2} \tag{5}$$

By substituting equation (5) into equations (1) and (2) and applying the trigonometric identity $\sin^2\alpha + cos^2\alpha = 1$. Under the narrowband assumption, we can apply superposition, to get the total power from the equal gain combiner by equation (6).

$$P_r 1 + P_r 2 = P_t \left(\frac{c\sqrt{G}}{2\pi f x}\right)^2 \tag{6}$$

Equation (6) can be analytically obtained if the two receiver antennas are vertically separated by a special metric $\Delta_h = h_{B1} - h_{B2}$ which can be determined by substituting expressions (3) and (4) into equation (5) simplifying it to

$$\frac{2h_{A1}h_{B1}}{x} - \frac{2h_{A1}h_{B2}}{x} = \frac{\lambda}{2} \tag{7}$$

Since $h_{A1} = h_{B1}$, we can apply the quadratic formula to equation (7) to get an explicit expression for $\Delta_h$.

$$h_{B1} - h_{B2} = \frac{\sqrt{{h_{B2}}^2 + \lambda x}}{2} - \frac{h_{B2}}{2}$$

$$\therefore \quad \Delta_h = \frac{-h_{B2} + \sqrt{{h_{B2}}^2 + \lambda x}}{2} \tag{8}$$

Expression (8) provides a way to determine the vertical antenna separation $\Delta_h$, i.e., if the location of the receiver node B is $x$ $(m)$, the carrier wavelength is $\lambda$, then for fixed applications in open space one can determine the optimal antenna separation given the height of the shortest receive antenna.

### 2.1 Variations In Node Heights Due To Meteorological Factors

In the preceding section we have analysed an ideal scenario between two fixed nodes when the sea was relatively calm. However, meteorological factors such as turbulence, tidal waves and rogue waves may create periodic fluctuations in the node heights. In general the variations in node heights directly affects the path differences $\Delta_x 1$ *and* $\Delta_x 2$ [14] and [13]. Let $h_{A1}+\epsilon_A$ , $h_{B1}+\epsilon_B$ *and* $h_{B2}+\epsilon_B$ be the effective vertical antenna placements above the mean sea level caused by variations in the meteorological factors affecting the sea. We can modify expression (3) to account for these changes such that $\Delta_x 1 = \frac{2(h_{A1}+\epsilon_A)(h_{B1}+\epsilon_B)}{x}$. After evaluating $\Delta_x 2$ in expression (4) in the same way, we can substitute the two modified expressions for path differences into equation (7). We then simplify to get a suboptimal vertical dynamic separation of the receiver antennas in presence meteorological disturbances $\Delta_{h_A}$ as shown in expression (9).

$$\frac{2(h_{A1}+\epsilon_A)(h_{B1}+\epsilon_B)}{x} - \frac{2(h_{A1}+\epsilon_A)(h_{B2}+\epsilon_B)}{x} = \frac{\lambda}{2}$$

$$\Delta_{h_A} = \frac{\lambda x}{4(h_{A1}+\epsilon_A)} \tag{9}$$

Expression (9) shows that if any meteorological factors affect the structural parameters of the two nodes, the variations in the node height around the receiver analytically cancel out. While the disturbances around the transmitter due to $\epsilon_A$ will have a significant impact to the value of $\Delta_{h_A}$. It is trivial to notice that if $\epsilon_A = 0$ and $h_{A1} = h_{B1} \neq 0$ then expressions (8) and (9) are algebraically equivalent.

## 3 Simulations Results

### 3.1 Simulation Model Description

We developed a numerical model to simulate SIMO from equation (6) using Matlab. In the first scenario we computed the received power $Pr1 \ (dBm)$ and $Pr2 \ (dBm)$ individually from expressions (1) and (2) across the coverage distance interval $\{800m \leq x + \delta_x \leq 1200m\}$, where $(\delta_x)$ is numerically equal to $Euler's\ number\ (e)\ metres$. Other system configurations considered were as follows: the receiver was located at a distance 1 $km$ away from the transmitter, the carrier frequency $f = 5.73\ GHz$, Effective Isotropic Radiated Power $EIRP = 30\ dBm$ and the shortest receiver antenna is mounted at 100 $m$. We combined the two received waveforms at a receiver with two antennas spaced according to $\Delta_h$ as derived in the ideal scenario in section 2. Hence from equation (8), the two receiver antennas were considered to be separated by $\Delta_h = 13.06cm$.

### 3.2 Spatial Diversity Simulation Under Calm Sea Conditions

Fig. 2, illustrates the received power at the desired location for three different antenna spacings. In legacy spatial diversity schemes, a rule of thumb is to separate the antennas by an integral product of half the wavelength. It's observed that if

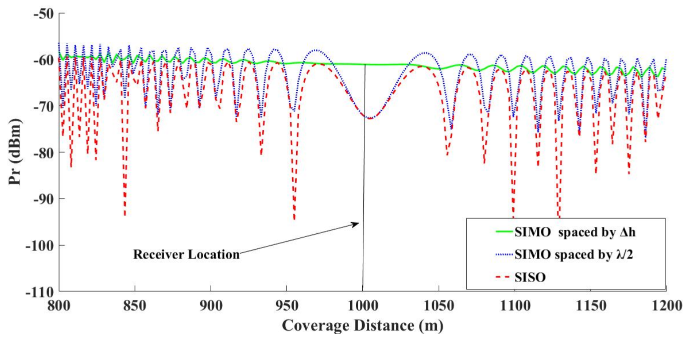


**Fig. 2.** Received Power for three different antenna spatial diversity configurations

the antennas are separated by half the wavelength, the destructive interaction of the reflected and direct paths is restored and the fast fading effects are restored at the receiver location. This is illustrated by a SIMO model with the two receiver antenna separated by $\frac{\lambda}{2}$ in fig. 2 which follows the same fading trend similar to Single Input Single Output (SISO). Comparing the received power at the desired location to the alternative spacing by the best current practice, fig.3 shows that if the receiver antennas are vertically separated by $5 \times \frac{\lambda}{2}$, the effects of fading are mitigated similar to the optimum $\Delta_h$ spacing in the ideal scenario illustrated in fig. 2. Although in this scenario we numerically multiplied by 5 after trying several iterations, it can be shown that this particular number is a consequence of expression (9) when $\epsilon_A = 0$ such that, $\Delta_{h_A} = \frac{\lambda x}{4h_{A1}} = \frac{\lambda}{2} \times \frac{1000}{4 \times 100.1306}$.

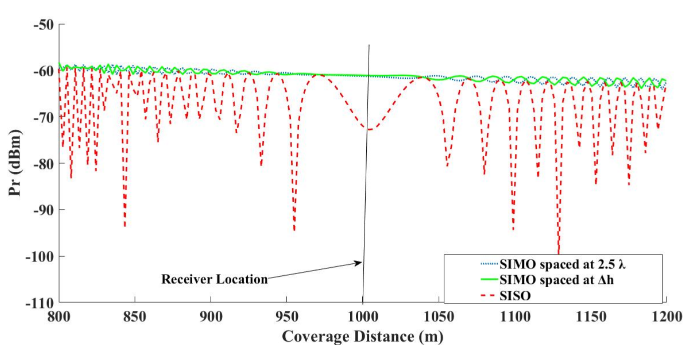


**Fig. 3.** SIMO with $\Delta_h$ Spacing SIMO with $5 \times \frac{\lambda}{2}$ Spacing

### 3.3 Counteracting Fading In Adverse Conditions

To demonstrate the effects of meteorological factors which affect mainly the reflected path by changing the relative node heights, we inserted the variations in the node height ($\epsilon_A$ *and* $\epsilon_B$) as defined in section 2.1. Fig. 4 shows the outcome of our simulation when there's a disturbance $\epsilon_B = -3m$ around the receiver location. It is evident that the SIMO model with $\Delta_h = 13.06cm$ remains unaffected by fast fading in a region of up to $50m$ away from the desired location. In order to demonstrate the extent of the deep fades we add the Friis Model [14], which predicts the maximum possible received power if the sea surface reflections are not affecting the LOS path of a SISO model.

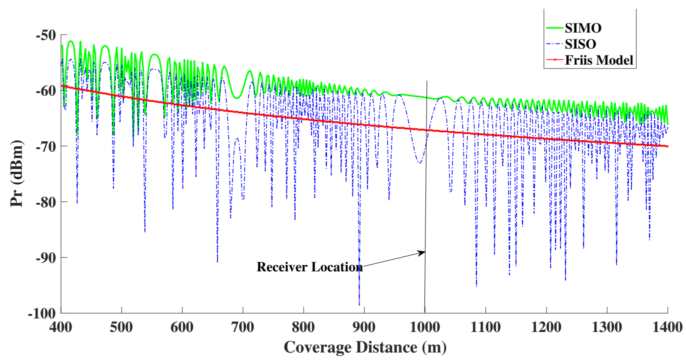


**Fig. 4.** SIMO, SISO, Friis Model: when node B is shorter by $3m$ above average sea level

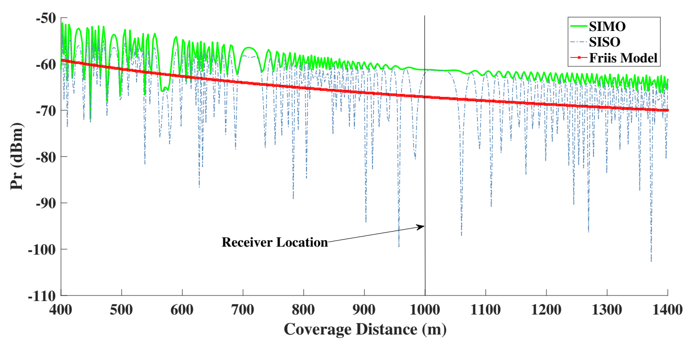


**Fig. 5.** SIMO, SISO, Friis Model: when node A is $3m$ more than its original height.

Fig.5 shows the effect of a disturbance in the sea surface which makes the transmitter apparently $3m$ taller. It is evident that the SISO model exhibits big difference in the received power around the receiver location. While the SIMO model remains almost flat at the receiver location with slower fading as we move away from the transmitter which is almost mirror effect to the observation in fig. 4. For the initial range of from $x = 800m \ to \ x = 1200m$, it was the received power from the SIMO model with $\Delta_h = 13.06cm$ is almost always above the Friis Model prediction and there are no deep fades with in this range.

## 4 Discussion and Conclusion

Due to the lack of multiple independent paths in the offshore environment it may not be possible to assume Rayleigh or Riccan statistics [15]. Therefore some of the latest Beamforming techniques aren't directly applicable in the mitigation of the deep fading in this environment. In this paper we applied a deterministic solution, but with the same objective and underlying mechanism i.e., varying the propagation phases in such a way, that the received signal at node B is optimised. Having independently developed our analytical SIMO model with $\Delta_h$ spacing, we found two other models for different applications from which one can draw comparisons to our model. A space and frequency hybrid diversity model was proposed by [16]. This model follows a different mathematical derivation but predicts the same results given the same inputs and system design considerations. For analytical comparisons we refer the reader to equations (3 and 4 in [16]). Another model derivation in rich multipath environment which included a strong LOS was demonstrated for a $2 \times 2$ short range indoor MIMO system with a transmitter-receiver node separation of about $x = 3m$ by [17].

Furthermore, the model which was presented in this report aimed to give a precise explicit way to determine the vertical spatial diversity of the receiver antennas in a $1 \times 2$ SIMO system for long-range point-to-point links wherever the two-ray model is applicable. Our system basically operates in a Single Input Multiple Output mode (SIMO), with the capability to implement a space-time scheme similar to the Alamouti code [18], resulting into a full $2 \times 2$ MIMO, which can improve the link capacity.

In the turbulent sea scenario we developed a suboptimal model $\Delta_{h_A}$ in expression (9) when $\epsilon_A \neq 0$. The two models $\Delta_{h_A}$ and $\Delta_h$ converge when $\epsilon_A = 0$ this condition remains true until the shortest receiver antenna is only a few wavelengths above the sea surface in order to avoid surface waves [14]. Thus, if the disturbances are localised at the receiver location the received signal is predicted to remain steady as long as none of the antennas are submerged. Moreover, the suboptimal model also demonstrates that a failure in the model is most likely to emerge from the disturbances closer to the transmitter which what one would expect from a spatial diversity SIMO since there is no transmit diversity. There are a few subtle differences between the two expressions (8) and

(9) namely: expression (9) has a pole at $\epsilon_A = -h_{A1}$ which means the model would breakdown if the transmitter gets closer to being submerged. $\Delta_h \to 0 \ \ as \ \ h_B \to \infty$ which intuitively means that the significance of the diversity will be reduced if the receiver node is extremely high. $\Delta_{h_A} \to 0 \ \ as \ \ h_A \to \infty$ implies that if the transmitter is extremely high again the significance of spatial diversity in such an environment will be reduced. Moreover, expression (9) is also applicable when the two nodes are asymmetrically designed such that $h_{A1} \neq h_{B1}$.

### 4.1 Conclusion

The mitigation of sea surface reflection through channel modelling has been demonstrated analytically and through extensive simulated results. Sea surface reflections are the main source of distortion in propagating electromagnetic waveforms experienced in the maritime wireless communications. In legacy systems, low frequency RF transceivers are normally deployed for this environment. We have demonstrated, how a steady link for fixed applications can be constructed in the Microwave band.

Particularly for turbine-to-turbine links in an offshore wind farm, one can avoid the problems which emerge from the sea surface reflections by mounting the antenna extremely high above the sea surface. Since turbines in this environment can reach up to 100 metres high. Alternatively, highly directive antenna can be utilised to ensure that the transmitted beam never reaches the sea surface. We have bypassed both these approaches and proposed a design which does not greatly depend on either antenna height or high directivity to counteract the fading in this environment. Further more, we have illustrated that the rule of thumb antenna spacing method implemented by separating the antennas by several wavelengths, asymptotically approaches the performance of our model. Moreover, the developed model exhibits a considerable resilience to fast fading across a long coverage distance away from the desired location. There is a possibility of extending this model to counteract fading in mobile maritime applications.

## References


1. Agarwal, D. and Kishor, N.: Network lifetime enhanced tri-level clustering and routing protocol for monitoring of offshore wind farms in IET Wireless Sensor Systems, Volume: 4, Issue: 2, pp. 69 ? 79. (2014).
2. Reyes-Guerrero, J. C. *et al.*: Measuring and Estimating the Propagation Path Loss and Shadowing Effects for Marine Wireless Sensor Networks at 5.8 GHZ. in 20th Telecommunications forum TELFOR 2012, pp. 323 ? 326. (2012).
3. ITU.: Reflection from the surface of the Earth. ITU REP. 1008-1, pp 75 ? 82. ITU, (1986).
4. Macmillan, A.*et al.*: Slow Frequency Hopping for Mitigating Tidal Fading on Rural Long Distance Over-Water Wireless Links INFOCOM IEEE Conference on Computer Communications Workshops San Diego, CA, USA, pp 1 ? 5, (2010).

5. Gordon, A. L. *et al.*: Tide PHYSICS URL https://www.britannica.com/science/tide. ONLINE Accessed 7th Jan 2017.(2018)
6. Doong D. and Wu L.: Searching for freak waves from in-situ buoy measurements OCEANS 2010 IEEE - Sydney, IEEE Conferences, pp 1?6 (2010). DOI: 10.1109/OCEANSSYD.2010.5603633
7. Lee, Y. H. and Meng, Y. S.: Key Considerations in the Modeling of Tropical Maritime Microwave Attenuations. International Journal of Antennas and Propagation,vol 2015, Article ID 246793, pp. 1 ? 7. (2015).
8. Salehinejad, H. *et al.*: PPM-UWB channel modeling for SCADA communications in Offshore Wind Farms Iranian Conference on Smart Grids, pp. 1 ? 6. (2012).
9. Anaya-Lara, O. *et al.*: Communications Requirements and Technology for Wind Farm Operation and Maintenance. First International Conference on Industrial and Information Systems, pp. 173 ? 178. (2006).
10. Hussain, S. and Kim, Y.: Simulation studies of resilient communication network architecture for monitoring and control wind power farms. International Conference on Advanced Communication Technology (ICACT), pp. 653 ? 658. (2015).
11. Hussain, S. and Kim, Y.: Fault resilient communication network architecture for monitoring and control of wind power farms 18th International Conference on Advanced Communication Technology (ICACT), pp. 685 ? 692. (2016)
12. Garroppo, R. G. *et al.* : Experimental and Simulation Study of a WiMAX System in the Sea Port Scenario in Proc IEEE International Conference on Communications, pp. 1 ? 5. (2009).
13. Reyes-Guerrero, J. C. *et al.*: Buoy-to-ship experimental measurements over sea at 5.8 GHz near urban environments. in Proc IEEE 11th Mediterranean Microwave Symposium. (MMS), pp. 320 ? 324. (2011)
14. Goldsmith, A.: Path Loss and Shadowing. Wireless Communications, pp 30 ? 31 Cambridge: Cambridge University Press, (2005).
15. Ferrand, P. Yang, S.: Blind precoding in line-of-sight MIMO channels. Signal Processing Advances in Wireless Communications (SPAWC) 2016 IEEE 17th International Workshop on, pp. 1?5, (2016).
16. Garcia-Lopez, J. Ferrandiz, J. and Selga, J. : Design of hybrid diversity on over-water paths. IET Journals & Magazines, Electronics Letters, Volume: 18, Issue: 10, 420 ? 422, (1982).
17. Sarris, I. and Nix, A. : Design and performance assessment of high-capacity MIMO architectures in the presence of a line-of-sight component. IEEE Trans. Veh. Technol., vol. 56, no. 4, pp. 2194 ? 2202, (2007)
18. Alamouti, S. : A simple transmit diversity technique for wireless communications. IEEE Journal on Selected Areas in Communications. 1451?1458 (1998).